IEEE Access
Multidisciplinary ⋮ Rapid Review ⋮ Open Access Journal

Received September 7, 2021, accepted October 13, 2021, date of publication October 26, 2021, date of current version November 1, 2021.

Digital Object Identifier 10.1109/ACCESS.2021.3122935

Thin Piezoelectric Mobile Robot Using Curved Tail Oscillation

HYEONJUNG LIM[1,2], SEUNG-WON KIM[1], (Member, IEEE), JAE-BOK SONG[2], (Senior Member, IEEE), AND YOUNGSU CHA[3], (Senior Member, IEEE)

[1]Center for Healthcare Robotics, Korea Institute of Science and Technology, Seoul 01811, Republic of Korea
[2]School of Mechanical Engineering, Korea University, Seoul 02841, Republic of Korea
[3]School of Electrical Engineering, Korea University, Seoul 02841, Republic of Korea

Corresponding author: Youngsu Cha (ys02@korea.ac.kr)

This work was supported in part by the National Research Foundation of Korea (NRF) through the Ministry of Science and ICT (MSIT), Korean Government under Grant 2020R1A2C2005252; and in part by the Korea University under Grant K2106631.

ABSTRACT In this paper, a novel piezoelectric material-based soft mobile robot is proposed. The robot consists of a thin film body and a soft polyvinylidene fluoride-based tail. The tail has a unique structure that is a combination of a polyethylene terephthalate fin and a curved piezoelectric film. We experimentally demonstrated the performance of a mobile robot. In particular, the resonance frequency was investigated to maximize tail movement. In addition, a parameter study of the tail shape was performed. Moreover, the repeatability of movements was tested. By using a curved piezoelectric tail with a fin, we built a mobile robot with a thin and flexible body. Furthermore, we fabricated multiple mobile robots by varying the robot configuration and analyzing their mobility. We found that our novel curved tail structure has good mobility performance at low body weights and multi-tailed conditions.

INDEX TERMS Piezoelectric material, mobile robot, soft robot.

I. INTRODUCTION

Soft robotic systems of various forms have been proposed as a systematic solution to perform tasks that require flexible manipulation and adaptive handling skills [1]–[3]. For instance, robotic grippers that integrate pneumatic systems with soft end-effectors as well as untethered robots with infinite degrees of freedom have been reported as solutions to grasp fragile objects and walk through rough terrain, respectively [4], [5]. By taking advantage of their material properties, the lack of adaptability of conventional robots arising from the kinematic constraints of their rigid structures can be overcome [6], [7].

Soft mobile robots are an important field of soft robotic systems. Compared to previously reported conventional mobile robots that mainly utilize wheels [8], [9] or pneumatic systems [10] for the mobility, soft mobile robots have broader options to achieve mobility [11], [12], such as chemical reactions [13], [14] and the actuation of the materials [15], [16]. Realizing robot mobility using chemical reactions or actuation of materials can improve the portability, and smart materials can act as a perfect medium for inducing an acceleration owing to their material properties [17]–[19]. Their advantages such as self-responsiveness [20], [21], flexibility [22], and light weight [23], enable smart materials to change the conventional definition of robots. For instance, a soft robotic actuator [24] that can morph its shape depending on the surrounding environment using ionic polymer metal composites has been reported. Various types of smart materials exist, and piezoelectric materials are among the most representative of them owing to their piezoelectric characteristic, which is a coupled response between mechanical stress and electrical charge. Specifically, since piezoelectric material has fine electro-mechanical coupling coefficient, light-weight, and good frequency response over other smart material counterparts [25]–[27], piezoelectric materials can be actuated under the reasonable input voltage having low power or high frequency [28]. Thus, piezoelectric materials can be used to generate thrust needed for soft mobile robots [29], [30]. Among various piezoelectric materials, polyvinylidene fluoride (PVDF) is a representative one [31]. Because PVDF is more flexible than its counterparts with good piezoelectric characteristics [32], PVDF has been widely utilized for a soft robotic platform. For instance, a soft

The associate editor coordinating the review of this manuscript and approving it for publication was Hui Xie.

mobile robot which moves through oscillation of PVDF [33] has been reported. A PVDF-based soft robotic platform enabled the robot to mimic the running motion of the animal and was also capable of fast motion of up to 70 % of its body length in a second. In this work, a thin piezoelectric mobile robot using curved tail oscillation is proposed as a follow-up study.

Figure 1 illustrates the concept of a thin piezoelectric mobile robot with a curved tail. Compared to a previous publication [33], the robot is turned upside down. Interestingly, the leg in [33] is redesigned to form a tail. By relocating the actuating part from the body to tail, the legged body part can be fabricated in various shapes with multiple choices of materials. Also, the body part can be fabricated by light materials, which can improve energy efficiency of the robot. Thus, various versions of the proposed robots can be suggested. The main body is fabricated from polyethylene terephthalate (PET) instead of the piezoelectric material so that the robot can withstand wet surfaces due to the insulation afforded by the material. To generate thrust for mobility, we use the resonance of the piezoelectric structure as in previous studies that implement the movement of the mobile robot through the oscillation of the piezoelectric material [34], [35]. Similar moving mechanism that utilized vibration of the legged body part of the robot has been proposed as a toy, named as bristlebot. Compared to bristlebot that typically delivers thrust from tiny motors to bristles, the focus of our work was on proposing robotic structure that only consists of soft materials. The actuation from piezoelectric materials makes our robotic structure free from limitation in size. Additionally, the soft structure enables the robot to withstand and absorb the applied impact [5]. With these advantages, the effect of robot configurations in mobility is studied thoroughly by a series of experiments.

Our major contributions are as follows: (i) proposing a novel soft mobile robot mechanism based on a curved piezoelectric tail; (ii) conducting a systematic analysis of the oscillation of the curved piezoelectric tail; and (iii) studying the mobility characteristics of the mobile robot through a series of experiments.

The remainder of this paper is organized as follows. In section II, the detailed fabrication process of the thin piezoelectric mobile robot is presented. In section III, the experimental setup for studying the characteristics of the tail and mobile robot is established. In section IV, experimental results for the curved piezoelectric tail and thin soft mobile robot are described. Finally, the conclusions are presented in the last section.

II. FABRICATION PROCESS

The thin piezoelectric mobile robot consists of a soft tail and legged body. Specifically, the tail is a combined structure of the curved PVDF film and the PET fin. Additionally, the legged body is composed of a PET substrate. The actuation of the tail is realized using a PVDF film (Measurement Specialties Inc.) with a thickness of 28 μm. Figure 2 (a) illustrates

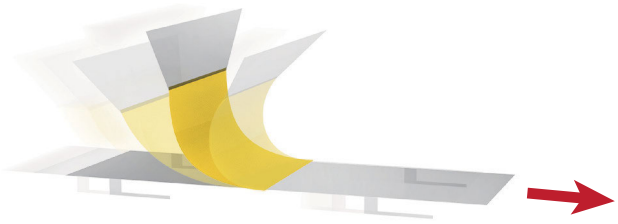

FIGURE 1. Thin piezoelectric mobile robot with curved tail.

the fabrication process for the PVDF part of the curved tail. First, the PVDF film was cut to 15 mm in length and 20 mm in width. Then, conductive epoxy (Epoxy adhesive 8331, M.G. Chemicals Ltd.) to improve the adhesion was applied to a small part on the upper right of the PVDF film, and copper tape (1181, 3M Co.) was attached to this area for the external wire connection. To create a curved structure, the PVDF film attached to the copper tape was combined with a pre-stretched Kapton tape (8997, 3M Co.). The remaining Kapton tape was cut to fit the PVDF film. We fabricated three types of PVDF tails with curvatures of 85 m^{-1}, 95 m^{-1}, and 115 m^{-1}. Second, the fin of the tail and legged body part of the robot were fabricated from PET film with a thickness of 100 μm. Figure 2 (b) displays the process of combining the PET components with the piezoelectric actuator. The fin of the tail and body parts of the robot were cut using a laser cutter (Mini 24, Epiloglaser). Specifically, the fin of the tail had a trapezoidal structure with an upper width, lower width, and height of 30 mm, 20 mm, and 10 mm, respectively. The fin was added to amplify the mobility of the robot. The legged body part had width and length of 15 mm and 50 mm, respectively. After laser cutting, the four legs of the body were folded at 90° to the body after the laser cutting. Finally, the curved PVDF layer was combined with the legged body part using epoxy glue (Epoxy Adhesive DP460, 3M Co.) at the center and cured for 24 h at 20 °C. In addition, the PET trapezoidal fin was attached to the curved PVDF film using double-sided PET tape with a thickness of 20 μm. The completed piezoelectric mobile robot with a curved tail after the fabrication process is shown in figure 2 (c).

III. EXPERIMENTAL SETUPS

A. MEASUREMENT OF TAIL OSCILLATION

To observe the movement of the curved tail according to the actuation of the piezoelectric material, we built a setup as shown in figure 3. To study the displacement of the tail, the partial area of the tail was clamped. Specifically, the partial area of the curved PVDF was bonded to the PET legged body. The displacement of the structure was measured using a 2D laser sensor (LJ-V7080, Keyence Co. Ltd.)

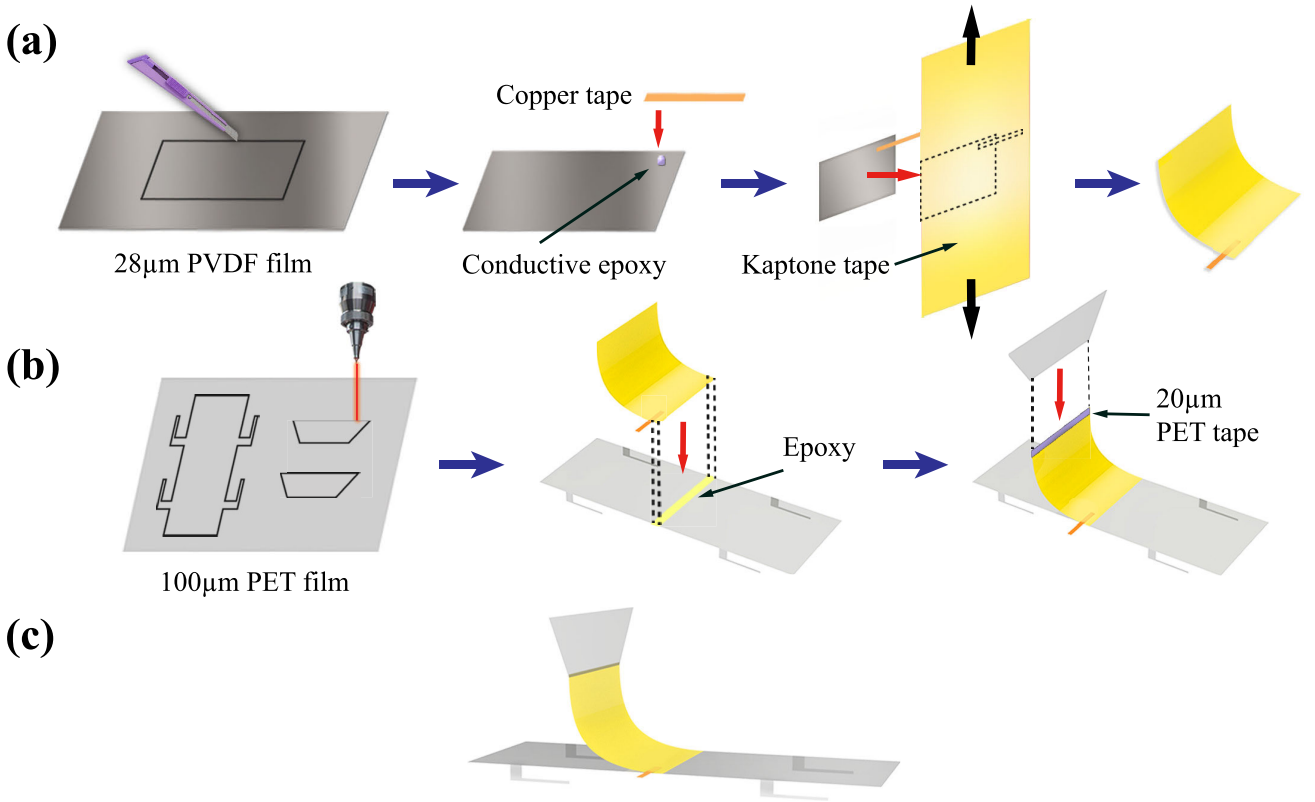

FIGURE 2. Schematic of fabrication process. Sequential order of fabricating thin piezoelectric mobile robot and its configurations are illustrated. (a) Fabrication process of curved PVDF film. (b) Combination of curved PVDF film with PET-based legged body part and fin of the tail. (c) Completion of thin piezoelectric mobile robot.

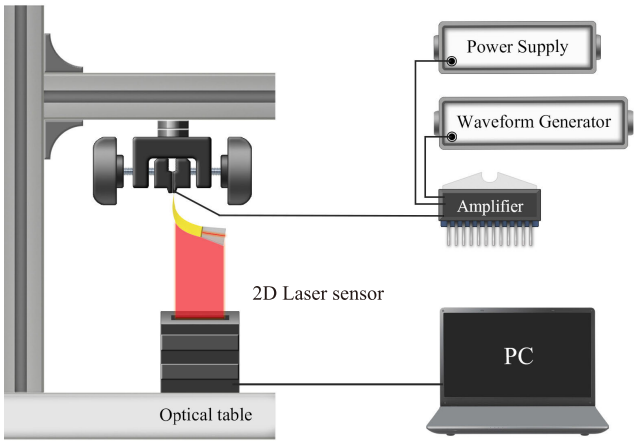

FIGURE 3. Experimental setup of laser displacement sensor for measuring the movement of piezoelectric tail.

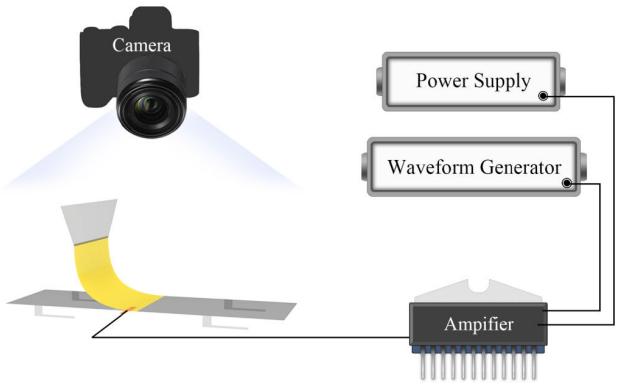

FIGURE 4. Experimental setup for observing the movement of the thin piezoelectric mobile robot.

placed under the tail. To supply the voltage input to the tail, we used a waveform generator (33500B, Keysight Technology), a power supply (MK-3003P, MK Power), and a voltage amplifier (PA95, Apex Microtechnology Co. Ltd.). The voltage amplifier was embedded in an evaluation kit (EVAL 23, REVB, Apex Microtechnology Co. Ltd.). A Teflon wrapping wire was used to apply the voltage by connecting the amplifier and the tail. The maximum peak-to-peak voltage amplitude was chosen based on the PVDF film datasheet and the preliminary test. We analyzed the oscillation of the tail along the longitudinal direction using the measured 2D laser sensor data.

B. MEASUREMENT OF ROBOT MOBILITY

Figure 4 illustrates the experimental setup used to observe the movement of the thin piezoelectric mobile robot. We utilized the same setup as in section III-A to apply the input voltage for robot operation. The mobile robot was tested on a PET surface. The movement of the robot was recorded

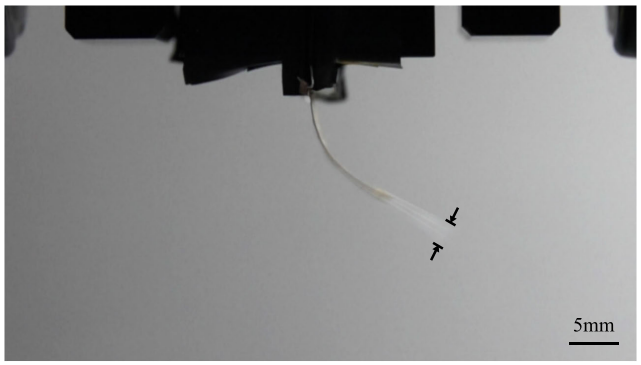

FIGURE 5. Time lapse of oscillation when a square wave with amplitude of 170 V and frequency of 49 Hz is applied to the curved piezoelectric tail.

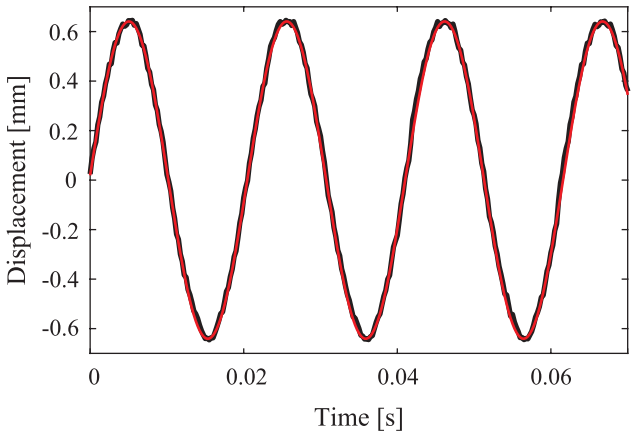

FIGURE 6. Time trace of displacement and sine-fitted result when a square wave with an amplitude of 170 V and the frequency of 49 Hz is applied to the curved piezoelectric tail. Black and red solid lines indicate displacement output of the PVDF and sine-fitted result, respectively.

using a camera (DSC-RX100M6, Sony Co.) with a frame rate of 30 fps and processed it to 2D displacement data by observing the movement of the marker at the center of the legged body. The movement of the trace marker from the recorded videos was extracted using a post-processing tracking program (ProAnalyst, Xcitex). The velocity of the mobile robot was calculated from the movement of the marker.

IV. RESULTS

A. ANALYSIS OF THE TAIL OSCILLATION

1) TAIL OSCILLATION

We applied a square wave with a peak-to-peak voltage amplitude of 170 V and frequency of 49 Hz. Figure 5 displays the representative time lapse of the oscillation of the curved tail with the fin. Figure 6 shows the representative displacement of the tip of the tail when a square wave with a peak-to-peak voltage amplitude of 170 V and frequency of 49 Hz was applied. The oscillation of the tail showed a high match with the sinusoidal wave with an R-square value of 0.9985. Thus, we extracted the amplitude of the displacement by applying sine fitting.

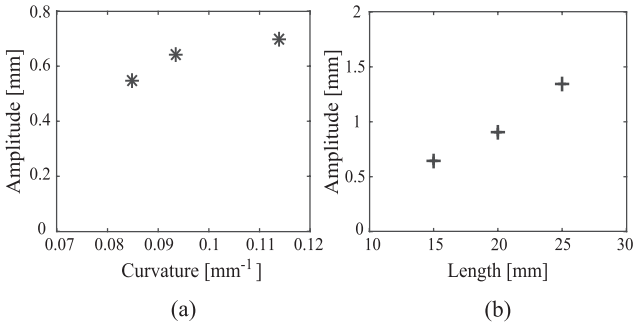

FIGURE 7. Displacement amplitude of the tail according to change in (a) curvature and (b) length of the curved PVDF.

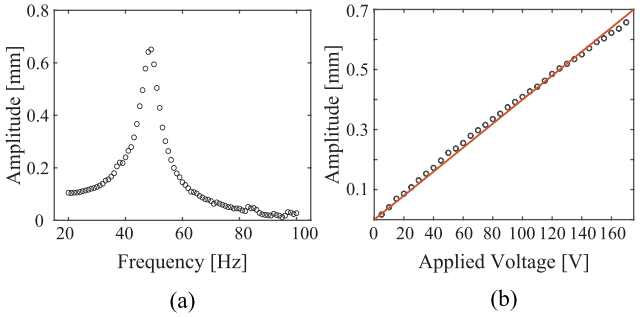

FIGURE 8. Extracted displacement amplitude according to the change in (a) frequency and (b) applied voltage. Black circles and red line indicate extracted amplitudes and linear fitting result, respectively.

2) TAIL SPECIFICATION

To study the effect of tail structure on the mobility of the robot, several tails with different parameters were tested. Specifically, we varied the curvature and longitudinal length of the curved PVDF and compared the oscillation amplitudes.

First, tails with curvatures of 85 m^{-1}, 95 m^{-1}, and 115 m^{-1} were prepared. They had a length of 15 mm. Then, using the experimental setup shown in figure 3, the displacement amplitude of the tail was extracted. Figure 7 (a) shows the extracted displacement amplitudes according to different curvatures. The curved angles of PVDF with reference to the clamped surface were 68°, 75°, and 93° for the tail with a curvature of 85 m^{-1}, 95 m^{-1}, and 115 m^{-1}, respectively. Based on the relationship between the curvature of the tail and the displacement, we found that the displacement increased with an increase in curvature. However, the increase of the displacement when the curvature changed from 95 m^{-1} to 115 m^{-1} reduced than the difference when the curvature changed from 85 m^{-1} to 95 m^{-1}. In addition, the case with a curvature of 115 m^{-1} exceeds 90°. Thus, for further experiments, we selected the curvature of the tail as 95 m^{-1}.

Also, we investigate the effect of the length of the curved tail. Aside from the curved PVDF with a longitudinal length of 15 mm, tails with lengths of 20 mm and 25 mm were fabricated. Using the setup shown in figure 3, we compared the displacement amplitude according to the change in the longitudinal length. Figure 7 (b) shows the displacement amplitudes with respect to the longitudinal length of the curved PVDF. We observed that the oscillation increased with

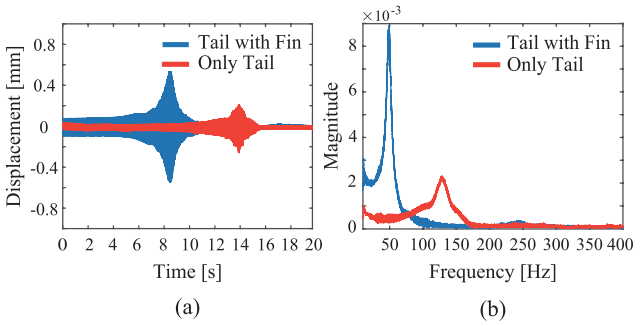

FIGURE 9. Displacement of the piezoelectric tail according to frequency sweep. (a) Time-traced displacement of the piezoelectric tails and (b) frequency response of displacement.

the length. We command that the increase in oscillation by a greater length results in more charge than a lesser longitudinal length [36]. Thus, the input energy for actuation increases with length. For further experiments, we utilized a curved PVDF with a longitudinal length of 15 mm.

3) RESONANCE OF THE TAIL

To determine the resonance frequency, we applied a square wave with a fixed peak-to-peak voltage amplitude of 170 V and a frequency that varies from 10 Hz to 100 Hz with a step of 1 Hz to the curved PVDF. Figure 8 (a) shows the extracted displacement amplitude according to the frequency change. Herein, we confirmed that resonance occurs when a square wave with a frequency of 49 Hz is applied to the tail. Thus, to maximize the oscillation of the tail under the given condition, we applied a square wave with a frequency of 49 Hz to the curved PVDF.

After determining the resonance frequency, the controllability of the fin was tested by applying input voltages with varying amplitudes, as depicted in figure 8 (b). Specifically, the peak-to-peak voltage amplitudes were varied from 5 V to 170 V in steps of 5 V. Herein, the oscillation amplitude of the fin increased linearly with an R-square value of 0.9952 according to the increase in the applied peak-to-peak voltage amplitude. Thus, under a given resonance frequency, the displacement of the tail can be controlled by adjusting the voltage.

4) EFFECT OF THE FIN

To determine the importance of the fin, we fabricated a tail without the PET fin. In addition, the frequency of the input voltage was swept from 10 Hz to 400 Hz. Figure 9 (a) shows the displacement results at the tip for both cases (with and without fins). We confirmed that the maximum displacement of the tail with the fin was amplified to approximately 2.5 times compared to the case without the fin. Additionally, we converted the time-traced displacements of the tip to frequency domain by performing a fast Fourier transform (FFT) [37] using MATLAB, as illustrated in figure 9 (b). In the frequency domain, the tail with the fin and the other case showed distinctive spectra. Specifically, the resonance

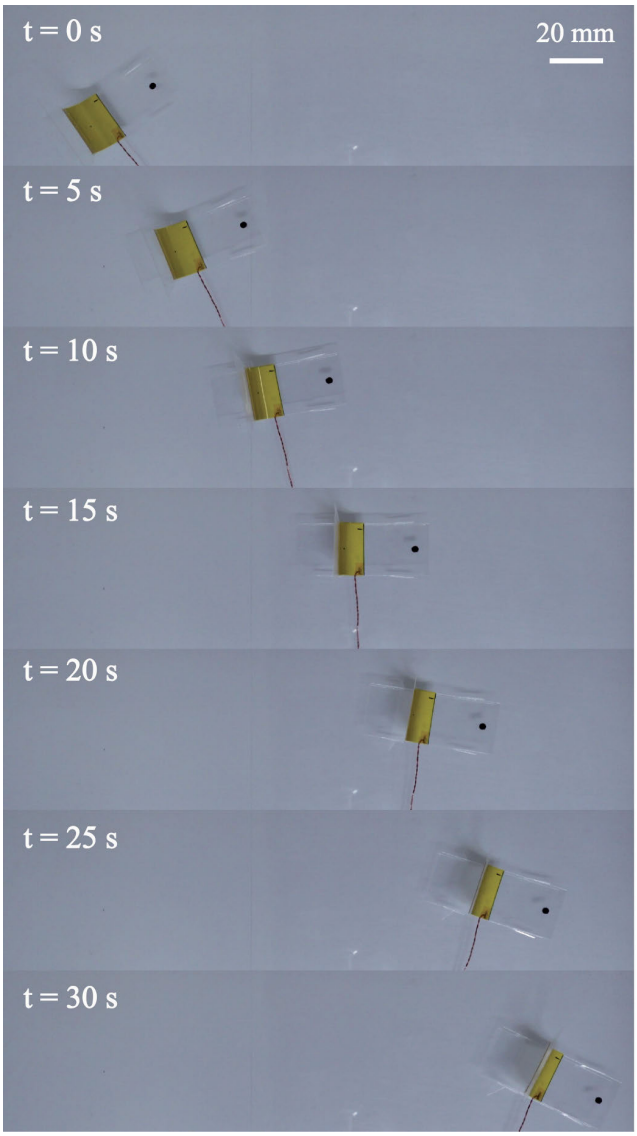

FIGURE 10. Time-traced picture of the mobility test of the thin piezoelectric mobile robot.

frequency of the curved tail with the fin diminished to 49 Hz compared with the other case of 119 Hz. To check the credibility of the FFT results, we simulated the resonance frequency of the curved tail without the fin using COMSOL Multiphysics 5.3a [33]. Through the numerical simulation in the two-dimentional space, the eigen value of the frequency response was obtained as 113 Hz. The simulated result by COMSOL showed a high match with the FFT output of the finless tail as shown figure 9 (b), with a discrepancy of 5 %. Thus, by performing FFT, credible information on the oscillation of the curved PVDF can be obtained. Additionally, the FFT output of the tail with the fin in figure 9 (b) can also be compared with the extracted frequencies illustrated in figure 8 (b). Because the trends of the FFT results showed good similarity, the reliability of the result can also be verified even in the finned condition. Furthermore, because a thin piezoelectric tail with a fin can be actuated with a comparably

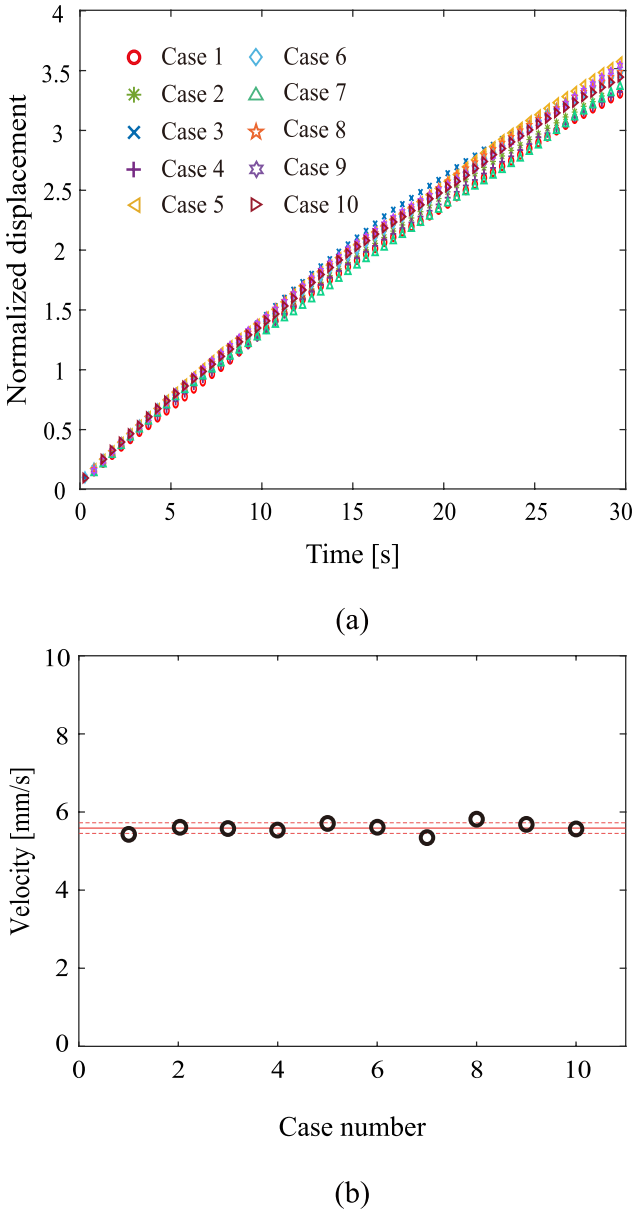

FIGURE 11. (a) Displacement variations of the thin piezoelectric mobile robot normalized with body length for ten cases and (b) average velocity according to the test cases. Red solid line, red dashed lines, and circles represent mean of average velocity, standard deviation of average velocity, and each average velocity, respectively.

lower operating frequency and a larger displacement than the other case, the fin plays an important role in the mobile robotic system [38], [39].

B. MOBILITY OF THE ROBOT

1) LOCOMOTION OF THE MOBILE ROBOT

Using the robot configuration in section II, the mobility test was performed with the experimental setup shown in figure 4. Figure 10 shows a representative time-traced mobility test. The movement of the robot was captured every 5 seconds. We note that the path of the robot was not straight but was in the form of an arc because of the tension of the

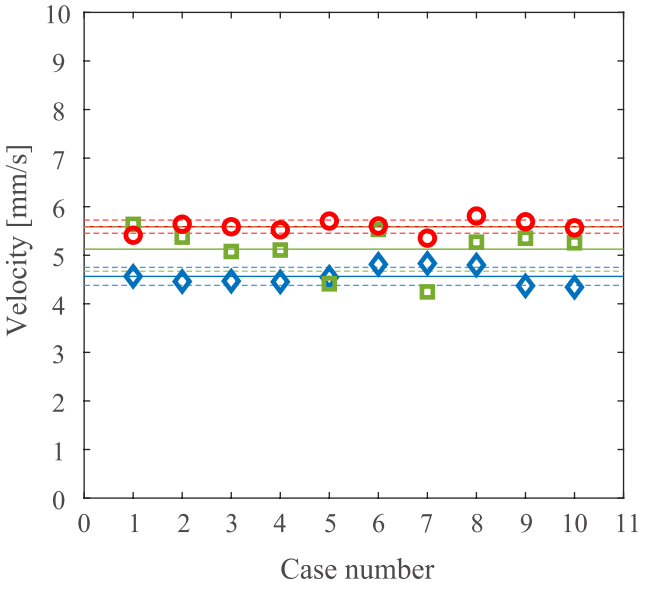

FIGURE 12. Average velocity and standard deviation of three identical thin piezoelectric mobile robots. Solid line, dashed lines, and markers represent mean of average velocity, standard deviation of average velocity, and each average velocity, respectively. Red, green, and blue colors are results from each mobile robot.

electric wire that was connected to the robot. The mobile robot moved approximately 170 mm in 30 seconds. The velocity of the robot is 5.6 mm/s. This is comparatively slower than that reported in a previous publication [33], [40]. To be specific, with 21 % less piezoelectric layer, the proposed mobile robot had lower average speed of 15 % compared to the prior study [33]. However, comparable slower speed might be attributed to distinct moving mechanism with the previous study. Considering that the proposed tailed robot delivers thrust from the tail to the body rather than actuation of the body itself, the robot shows slower moving speed than the prior research due to force delivery loss [41].

Repeated movability tests were performed to ensure repeatability. Specifically, we recorded the movements of the robot for 30 seconds for ten iterations. The displacements for the ten cases are illustrated in figure 11 (a). We commented that each displacement was normalized by the length of the body. The mobile robot exhibited a similar time-traced trajectory. The trajectories were then converted to the average velocity of the robot, as shown in figure 11 (b). The average velocity of the proposed mobile robot was 5.6 mm per second. The mobile robot took 8.9 seconds to move until its body length was covered. Thus, the robot is able to move by approximately 11.2 % of the body length.

Lastly, to study the variation of handmade fabrication on mobility, we made three identical robots. We then repeated the mobility test for ten cases for each mobile robot. Figure 12 shows the results of the mobility tests for the three identical robots. Herein, the robots had similar average velocities of 5.6 mm/s, 5.1 mm/s, and 4.6 mm/s.

TABLE 1. Material property of the legged body configuration.

Material	Size [mm^2]	Weight [g]	Thickness [mm]	Young's modulus [GPa]	Stiffness [mN/m]
Paper	50 × 20	0.08	0.10	6.82	90.93
PET 1	50 × 20	0.15	0.16	2.90	38.67
PET 2	60 × 20	0.18	0.16	2.90	22.38
PP	50 × 20	0.20	0.27	1.30	138.67

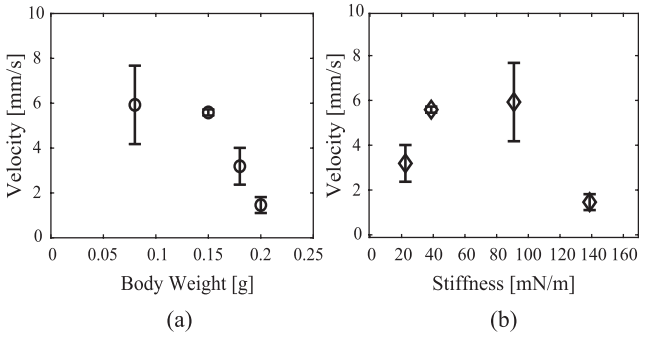

FIGURE 13. Mean and standard deviation of the average velocity according to the body material change. (a) Average velocity with respect to weight change and (b) stiffness change.

2) MATERIAL CHANGE IN LEGGED BODY PARTS

To investigate the effect of the legged body on the mobility, we fabricated different legged bodies with various materials. Ten repeated mobility tests were then performed. The size of the tail and fin were all identical, and the materials used for the body were paper, PET film, and polypropylene (PP). Young's moduli of each material are 6.82 GPa, 2.9 GPa, and 1.3 GPa for paper [42], PET [43], and PP [44], respectively. Additionally, a PET body with a longitudinal length of 60 mm was fabricated to compare the effect of body length on mobility. The movements of the thin piezoelectric mobile robots were then analyzed using the experimental setup shown in figure 4. The characteristics of the robots are listed in table 1. The stiffness of the body is obtained using Young's modulus × Moment of inertia / Length^3. From figure 13, we can observe that the different body weights and stiffnesses of different materials affected the velocity. Specifically, we found an inverse relationship between the weight and velocity. In addition, the longer PET body resulted in a lower velocity due to the increased weight. Moreover, the velocity and stiffness did not have a unique relation.

3) MULTI-TAIL OPERATION

We added an additional tail to the mobile robot to study the effect of multiple tails. Two tails were attached at 15 mm and 35 mm from the front of the body. We comment that the other conditions remained the same as the one-tailed mobile robot. Subsequently, ten repeated mobility tests were performed. Figure 14 shows the average velocity when an additional tail is added to the robot. Consequently, the average velocity of the mobile robot with two tails was 1.2 times faster than the original robot. Interestingly, the robot with two tails took 7.2 seconds to traverse its body length.

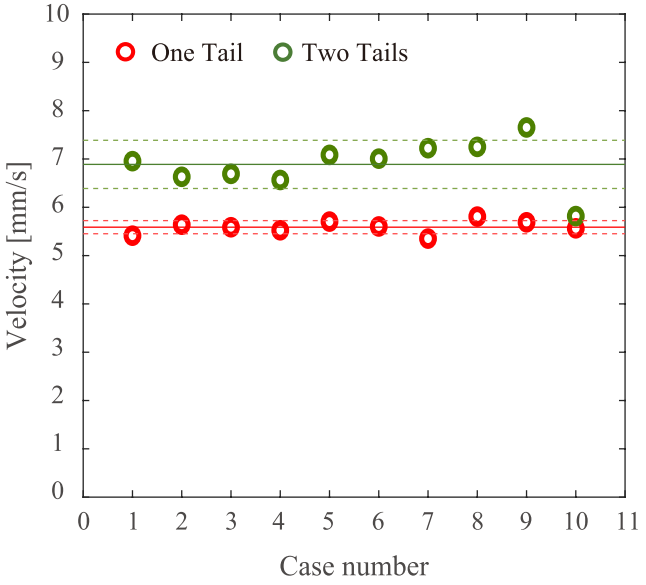

FIGURE 14. Average velocity of the thin piezoelectric mobile robots with single and double tails, respectively. The solid line, dashed lines, and circles represent the mean of average velocity, standard deviation of average velocity, and average velocity, respectively. Red and green indicate the average velocities of the single- and double-tailed piezoelectric robots, respectively.

V. CONCLUSION

We propose a novel soft mobile robot that moves based on the oscillation of its tail. The soft mobile robot consists of a curved PVDF-based tail and a customizable body, and a fin attached to the tail oscillates such that the robot can move forward. The mobility of the robot was implemented by thrust through the resonance of the PVDF film, and PET film-based fin that can amplify the movement.

To study the movement characteristics of the thin piezoelectric mobile robot, we focused on the effect of the tail and legged body on the mobility. Specifically, to determine the effect of the curved PVDF on the mobility, we determined the optimal curvature and length of the tail. Then, the resonance frequency was obtained and analyzed for the effect of the fin on the curved PVDF. In addition, for the body part, we fabricated a legged body part with different materials to study the effect of the material on the mobility. In summary, the proposed robot can move at an average velocity of 5.6 mm per second, which indicates that it can move 11.2 % of its body length per second under experimental conditions. The repeatability of the robot under an identical experimental setup was also tested through repeated experiments. The robot showed similar movements for different test cases and was comparably free from fluctuations. In addition, with the

additional fin, we confirmed that there is even more room for the robot to improve its mobility.

Owing to its softness and flexibility, it is anticipated that the proposed mobile robot can perform tasks in harsh environments such as narrow passages or wet areas. In addition, its flexibility makes it possible to recover quickly from impact. In addition, apart from the advantages of the robot such as flexibility and small size, the greatest strength of the proposed robot lies in its adaptability. Because the body parts are easily customizable with any materials, different forms of the proposed robot can be suggested to adapt to various environments. Using these advantages, we hope that the proposed robot can be adapted to a soft rover to perform difficult tasks, such as space missions [45], [46].

Future works are to investigate the moving performance at various conditions such as the effect of the friction on different surfaces and to develop an independent robotic platform by including an embedded board and a battery without external wires.

REFERENCES

[1] M. Trumić, K. Jovanović, and A. Fagiolini, "Decoupled nonlinear adaptive control of position and stiffness for pneumatic soft robots," *Int. J. Robot. Res.*, vol. 40, no. 1, pp. 277–295, Jan. 2021.

[2] L. Qin, Y. Tang, U. Gupta, and J. Zhu, "A soft robot capable of 2D mobility and self-sensing for obstacle detection and avoidance," *Smart Mater. Struct.*, vol. 27, no. 4, Apr. 2018, Art. no. 045017.

[3] M. Shen, "A review paper of bio-inspired environmental adaptive and precisely maneuverable soft robots," 2021, *arXiv:2101.03171*.

[4] Y. Kim and Y. Cha, "Soft pneumatic gripper with a tendon-driven soft origami pump," *Frontiers Bioeng. Biotechnol.*, vol. 8, p. 461, May 2020.

[5] M. T. Tolley, R. F. Shepherd, B. Mosadegh, K. C. Galloway, M. Wehner, M. Karpelson, R. J. Wood, and G. M. Whitesides, "A resilient, untethered soft robot," *Soft Robot.*, vol. 1, no. 3, pp. 213–223, Sep. 2014.

[6] J. Borenstein, "Control and kinematic design of multi-degree-of freedom mobile robots with compliant linkage," *IEEE Trans. Robot. Autom.*, vol. 11, no. 1, pp. 21–35, Feb. 1995.

[7] A. Betourne and A. Fournier, "Kinematics, dynamics and control of a conventional wheeled omnidirectional mobile robot," in *Proc. IEEE Syst. Man Cybern. Conf. (SMC)*, vol. 2, Oct. 1993, pp. 276–281.

[8] J. Liao, Z. Chen, and B. Yao, "Model-based coordinated control of four-wheel independently driven skid steer mobile robot with wheel–ground interaction and wheel dynamics," *IEEE Trans. Ind. Informat.*, vol. 15, no. 3, pp. 1742–1752, Mar. 2019.

[9] W. E. Dixon, D. M. Dawson, E. Zergeroglu, and A. Behal, "Adaptive tracking control of a wheeled mobile robot via an uncalibrated camera system," *IEEE Trans. Syst. Man, Cybern. B, Cybern.*, vol. 31, no. 3, pp. 341–352, Jun. 2001.

[10] M. Polishchuk, M. Tkach, I. Parkhomey, J. Boiko, and O. Eromenko, "Experimental studies on the reactive thrust of the mobile robot of arbitrary orientation," *Indonesian J. Electr. Eng. Informat.*, vol. 8, no. 2, pp. 340–352, May 2020.

[11] S. Chen, Y. Cao, M. Sarparast, H. Yuan, L. Dong, X. Tan, and C. Cao, "Soft crawling robots: Design, actuation, and locomotion," *Adv. Mater. Technol.*, vol. 5, no. 2, Feb. 2020, Art. no. 1900837.

[12] D. Kim, J. I. Kim, and Y. Park, "A simple tripod mobile robot using soft membrane vibration actuators," *IEEE Robot. Autom. Lett.*, vol. 4, no. 3, pp. 2289–2295, Jul. 2019.

[13] C. D. Onal, X. Chen, G. M. Whitesides, and D. Rus, "Soft mobile robots with on-board chemical pressure generation," in *Robotics Research*. Cham, Switzerland: Springer, 2017, pp. 525–540.

[14] Y. Nishikawa and M. Matsumoto, "A design of fully soft robot actuated by gas–liquid phase change," *Adv. Robot.*, vol. 33, no. 12, pp. 567–575, Jun. 2019.

[15] J. Sohn, G.-W. Kim, and S.-B. Choi, "A state-of-the-art review on robots and medical devices using smart fluids and shape memory alloys," *Appl. Sci.*, vol. 8, no. 10, p. 1928, Oct. 2018.

[16] S. Zheng, T. Park, M. C. Hoang, G. Go, C.-S. Kim, J.-O. Park, E. Choi, and A. Hong, "Ascidian-inspired soft robots that can crawl, tumble, and pick-and-place objects," *IEEE Robot. Autom. Lett.*, vol. 6, no. 2, pp. 1722–1728, Apr. 2021.

[17] S. Coyle, C. Majidi, P. LeDuc, and K. J. Hsia, "Bio-inspired soft robotics: Material selection, actuation, and design," *Extreme Mech. Lett.*, vol. 22, pp. 51–59, Jul. 2018.

[18] Q. Shen, T. Stalbaum, N. Minaian, I.-K. Oh, and K. J. Kim, "A robotic multiple-shape-memory ionic polymer–metal composite (IPMC) actuator: Modeling approach," *Smart Mater. Struct.*, vol. 28, no. 1, Jan. 2019, Art. no. 015009.

[19] Z. J. Patterson, A. P. Sabelhaus, K. Chin, T. Hellebrekers, and C. Majidi, "An untethered brittle star-inspired soft robot for closed-loop underwater locomotion," in *Proc. IEEE/RSJ Int. Conf. Intell. Robots Syst. (IROS)*, Oct. 2020, pp. 8758–8764.

[20] A. Vanangamudi, L. F. Dumée, E. D. Ligneris, M. Duke, and X. Yang, "Thermo-responsive nanofibrous composite membranes for efficient self-cleaning of protein foulants," *J. Membrane Sci.*, vol. 574, pp. 309–317, Mar. 2019.

[21] J. F. Hester, S. C. Olugebefola, and A. M. Mayes, "Preparation of pH-responsive polymer membranes by self-organization," *J. Membrane Sci.*, vol. 208, nos. 1–2, pp. 375–388, Oct. 2002.

[22] I. Kang, Y. Y. Heung, J. H. Kim, J. W. Lee, R. Gollapudi, S. Subramaniam, S. Narasimhadevara, D. Hurd, G. R. Kirikera, V. Shanov, M. J. Schulz, D. Shi, J. Boerio, S. Mall, and M. Ruggles-Wren, "Introduction to carbon nanotube and nanofiber smart materials," *Compos. B, Eng.*, vol. 37, no. 6, pp. 382–394, 2006.

[23] S. H. Hassan, L. H. Voon, T. S. Velayutham, L. Zhai, H. C. Kim, and J. Kim, "Review of cellulose smart material: Biomass conversion process and progress on cellulose-based electroactive paper," *J. Renew. Mater.*, vol. 6, no. 1, pp. 1–25, Jan. 2018.

[24] H. Kim, S.-K. Ahn, D. M. Mackie, J. Kwon, S. H. Kim, C. Choi, Y. H. Moon, H. B. Lee, and S. H. Ko, "Shape morphing smart 3D actuator materials for micro soft robot," *Mater. Today*, vol. 41, pp. 243–269, Dec. 2020.

[25] I. Patel and M. Uzun, "The requirement for piezoelectric smart material for current and future applications," *Sigma*, vol. 29, pp. 395–411, 2011.

[26] R. Sitharthan, M. Ponnusamy, M. Karthikeyan, and D. S. Sundar, "Analysis on smart material suitable for autogenous microelectronic application," *Mater. Res. Exp.*, vol. 6, no. 10, Aug. 2019, Art. no. 105709.

[27] K. B. Waghulde and D. B. Kumar, "Vibration analysis of cantilever smart structure by using piezoelectric smart material," *Int. J. Smart Sens. Intell. Syst.*, vol. 4, no. 3, pp. 353–375, 2011.

[28] L. Sui, X. Xiong, and G. Shi, "Piezoelectric actuator design and application on active vibration control," *Proc. Phys.*, vol. 25, pp. 1388–1396, Jan. 2012.

[29] A. G. Dharmawan, H. H. Hariri, G. S. Soh, S. Foong, and K. L. Wood, "Design, analysis, and characterization of a two-legged miniature robot with piezoelectric-driven four-bar linkage," *J. Mech. Robot.*, vol. 10, no. 2, Apr. 2018, Art. no. 021003.

[30] Z. Longlong and L. Chaodong, "Development of a eight-legged bionic robot using piezoelectric bimorph actuators," *Metrol. Meas. Techn.*, p. 5, 2018.

[31] P. Ueberschlag, "PVDF piezoelectric polymer," *Sensor Rev.*, vol. 21, no. 2, pp. 118–126, Jun. 2001.

[32] Y. R. Wang, J. M. Zheng, G. Y. Ren, P. H. Zhang, and C. Xu, "A flexible piezoelectric force sensor based on PVDF fabrics," *Smart Mater. Struct.*, vol. 20, no. 4, 2011, Art. no. 045009.

[33] T. Park and Y. Cha, "Soft mobile robot inspired by animal-like running motion," *Sci. Rep.*, vol. 9, no. 1, pp. 1–9, Dec. 2019.

[34] J. Hernando-García, J. L. García-Caraballo, V. Ruiz-Díez, and J. L. Sánchez-Rojas, "Motion of a legged bidirectional miniature piezoelectric robot based on traveling wave generation," *Micromachines*, vol. 11, no. 3, p. 321, Mar. 2020.

[35] S. A. Rios, A. J. Fleming, and Y. K. Yong, "Miniature resonant ambulatory robot," *IEEE Robot. Automat. Lett.*, vol. 2, no. 1, pp. 337–343, Jan. 2017.

[36] C. Lee and F. C. Moon, "Laminated piezopolymer plates for torsion and bending sensors and actuators," *J. Acoust. Soc. Amer.*, vol. 85, no. 6, pp. 2432–2439, Jun. 1989.

[37] J. Chung, H. Lim, M. Lim, and Y. Cha, "Object classification based on piezoelectric actuator-sensor pair on robot hand using neural network," *Smart Mater. Struct.*, vol. 29, no. 10, Oct. 2020, Art. no. 105020.

[38] Z. G. Zhang, N. Yamashita, M. Gondo, A. Yamamoto, and T. Higuchi, "Electrostatically actuated robotic fish: Design and control for high-mobility open-loop swimming," *IEEE Trans. Robot.*, vol. 24, no. 1, pp. 118–129, Feb. 2008.
[39] Z. Chen, S. Shatara, and X. Tan, "Modeling of biomimetic robotic fish propelled by an ionic polymer–metal composite caudal fin," *IEEE/ASME Trans. Mechatronics*, vol. 15, no. 3, pp. 448–459, Jun. 2010.
[40] Y. Wu, K. Y. Ho, K. Kariya, R. Xu, W. Cai, J. Zhong, Y. Ma, M. Zhang, X. Wang, and L. Lin, "PRE-curved PVDF/PI unimorph structures for biomimic soft crawling actuators," in *Proc. IEEE Micro Electro Mech. Syst. (MEMS)*, Jan. 2018, pp. 581–584.
[41] D. G. Yablon, J. Grabowski, and I. Chakraborty, "Measuring the loss tangent of polymer materials with atomic force microscopy based methods," *Meas. Sci. Technol.*, vol. 25, no. 5, May 2014, Art. no. 055402.
[42] T. Yokoyama and K. Nakai, "Evaluation of in-plane orthotropic elastic constants of paper and paperboard," in *Proc. SEM Annu. Conf. Expo. Exp. Appl. Mech.*, Jun. 2007, pp. 1505–1511.
[43] S.-G. Kim, N.-H. You, W. Lee, J. Y. Hwang, M. J. Kim, D. Hui, B.-C. Ku, and J. H. Lee, "Effects of the functionalized graphene oxide on the oxygen barrier and mechanical properties of layer-by-layer assembled films," *Compos. B, Eng.*, vol. 92, pp. 307–314, May 2016.
[44] *Matweb*. [Online]. Available: http://www.matweb.com
[45] M. Peck, "Soft-robotic rover with electrodynamic power scavenging. Phase 1; NIAC final report; [soft robotics and electrodynamic tethers]," Cornell Univ., Tech. Rep., 2016.
[46] B. Trimmer, "An interview with NASA principal investigator vytas SunSpiral: Expert opinion on the advantages and limitations of soft robotics," *Soft Robot.*, vol. 2, no. 2, pp. 51–58, Jun. 2015.

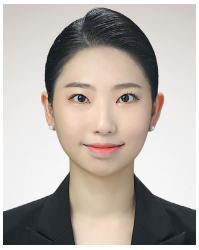

HYEONJUNG LIM is currently pursuing the M.S. degree in mechanical engineering from Korea University, Seoul, South Korea. She is currently a Student Researcher with the Center for Healthcare Robotics, Korea Institute of Science and Technology (KIST), Seoul. Her current research interests include soft actuator, wearable robotics, and smart materials and structures.

SEUNG-WON KIM (Member, IEEE) received the B.S. and Ph.D. degrees in mechanical and aerospace engineering from Seoul National University, Seoul, Republic of Korea, in 2009 and 2016, respectively. He was a Research Scientist with the Healthcare Robotics Group, Korea Institute of Science and Technology (KIST), from 2016 to 2018, where he is currently a Senior Research Scientist with the Center for Healthcare Robotics. He has been an Assistant Professor with the Department of AI-Robotics, University of Science and Technology (UST), since 2018. His research interests include bio-inspired robots, smart materials-based soft robotic mechanisms for medical, healthcare service, and wearable applications.

JAE-BOK SONG (Senior Member, IEEE) received the B.S. and M.S. degrees in mechanical engineering from Seoul National University, Seoul, South Korea, in 1983 and 1985, respectively, and the Ph.D. degree in mechanical engineering from MIT, Cambridge, MA, USA, in 1992. He joined as a Faculty Member of the Department of Mechanical Engineering, Korea University, Seoul, in 1993. His current research interests include the design and control of robot arms and gripper systems.

YOUNGSU CHA (Senior Member, IEEE) received the B.S. degree from Korea University, Seoul, South Korea, in 2004, and the M.S. degree from the Korea Advanced Institute of Science and Technology (KAIST), Daejeon, South Korea, in 2007, both in electrical engineering, and the Ph.D. degree in mechanical engineering from New York University, New York, NY, USA, in 2015. He was a Principal Research Scientist with the Center for Intelligent and Interactive Robotics, Korea Institute of Science and Technology (KIST), Seoul. He is currently an Assistant Professor with the School of Electrical Engineering, Korea University. His current research interests include smart materials and structures, multiphysics modeling, flexible sensors and actuators, energy harvesting, and robotics.